Geophysical Research Letters

RESEARCH LETTER
10.1029/2024GL109056

Processes that Contribute to Future South Asian Monsoon Differences in E3SMv2 and CESM2

Gerald A. Meehl[1], Christine A. Shields[1], Julie M. Arblaster[1,2], John Fasullo[1], Nan Rosenbloom[1], Aixue Hu[1], Richard Neale[1], Antonietta Capotondi[3], Jean-Christophe Golaz[4], Luke Van Roekel[5], and H. Annamalai[6]

[1]National Center for Atmospheric Research, Boulder, CO, USA, [2]ARC Centre of Excellence for Climate Extremes, Monash University, Melbourne, VIC, Australia, [3]CIRES and NOAA Physical Sciences Laboratory, University of Colorado, Boulder, CO, USA, [4]Lawrence Livermore National Laboratory, Livermore, CA, USA, [5]Los Alamos National Laboratory, Los Alamos, NM, USA, [6]IPRC/Department of Oceanography, University of Hawaii at Manoa, Honolulu, HI, USA

Abstract Two Earth system models are analyzed to gain insight into the processes that govern projected changes in the South Asian monsoon. Warmer present-day base state tropical SSTs contribute to coupled processes that produce greater future tropical Pacific warming in CESM2 with less of an increase in season-mean monsoon precipitation compared to E3SMv2. This is attributed to changes in the large-scale east-west atmospheric Walker circulation, with relatively larger increases in precipitation and upper-level divergence over the tropical Pacific and increases in upper-level convergence over South Asia in CESM2. The stronger El Niño-like response in CESM2, which increases Pacific precipitation and upper-level divergence farther to the east, and larger future ENSO amplitude in E3SMv2, produce a greater relative increase in future monsoon-ENSO connections in E3SMv2 compared to CESM2. This analysis indicates that the key processes that affect future monsoon-ENSO connections are ENSO amplitude and size of the future tropical Pacific El Niño-like response.

Plain Language Summary Two different Earth system models are analyzed to investigate processes that contribute to possible future changes of South Asian monsoon precipitation and connections to ENSO. The stronger increase of precipitation in CESM2 over the tropical Pacific, due in part to a larger El Niño-like response of Pacific SSTs, produces less of an increase in future monsoon precipitation in CESM2 compared to E3SMv2. The eastward shift of precipitation in CESM2, along with the larger increase of ENSO amplitude in E3SMv2, produce a stronger future monsoon-ENSO connection in E3SMv2 compared to CESM2.

Key Points:

- Warmer future tropical Pacific SSTs in CESM2 compared to E3SMv2 produce less of an increase in South Asian monsoon precipitation through the Walker Circulation
- Future monsoon-ENSO connections are stronger in E3SMv2 compared to CESM2 due to larger increases in future ENSO amplitude and shifts in the Walker Circulation
- Key processes that affect future monsoon-ENSO connections are ENSO amplitude and the size of the future tropical Pacific El Niño-like response

Supporting Information:

Supporting Information may be found in the online version of this article.

Correspondence to:

G. A. Meehl,
meehl@ucar.edu

Citation:

Meehl, G. A., Shields, C. A., Arblaster, J. M., Fasullo, J., Rosenbloom, N., Hu, A., et al. (2024). Processes that contribute to future South Asian monsoon differences in E3SMv2 and CESM2. *Geophysical Research Letters*, *51*, e2024GL109056. https://doi.org/10.1029/2024GL109056

Received 29 FEB 2024
Accepted 1 JUL 2024

Author Contributions:

Conceptualization: Gerald A. Meehl
Data curation: Nan Rosenbloom, Jean-Christophe Golaz
Formal analysis: Gerald A. Meehl, Christine A. Shields, Julie M. Arblaster, Antonietta Capotondi
Investigation: Gerald A. Meehl, Julie M. Arblaster, Nan Rosenbloom, Aixue Hu, Richard Neale, Antonietta Capotondi, Jean-Christophe Golaz, Luke Van Roekel, H. Annamalai
Methodology: Christine A. Shields, John Fasullo, Aixue Hu, Richard Neale

1. Introduction

Future South Asian monsoon precipitation has generally shown a summertime increase in a warmer climate in multi-model averages due to warmer tropical Indian ocean temperatures and greater moisture transport into the South Asian monsoon (Choudhury et al., 2022; Douville et al., 2000; Kripalani et al., 2007; Ueda et al., 2006; Varghese et al., 2020). Other factors that contribute to the precipitation increase seen in most CMIP models (Li & Ting, 2017; Mishra et al., 2020; Wu et al., 2022) include an increase in land-sea temperature contrast between southern Asia and the Indian Ocean (Kamae et al., 2014; Wu et al., 2022), which has been shown to be important for the magnitude of monsoon precipitation (e.g., Meehl, 1994), as well as related circulation and ITCZ displacement changes (Li et al., 2015). Decreases in land-sea temperature contrast were noted to contribute to decreases of South Asian monsoon precipitation up to the early 2000s (Roxy et al., 2015). But after that time an increase in land-sea temperature contrast was identified as being important for subsequent increases in monsoon precipitation (Jin & Wang, 2017; Roxy, 2017). Additionally, changes in atmospheric circulation could contribute to possible future decreases of monsoon precipitation in some regions (Ashfaq et al., 2009). For monsoon-ENSO connections, there is some evidence that a warmer climate could strengthen such connections if ENSO amplitude increases (Cai et al., 2022; Meehl et al., 2023) or if warmer base state tropical SSTs affect the Walker circulation (Bonfils et al., 2015; Katzenberger et al., 2021; McGregor et al., 2022; Meehl et al., 2023). However, the wide spread in model responses in the future strength of the monsoon-ENSO connection (e.g., Goswami & An, 2023; Li & Ting, 2015) indicates that additional insights must be obtained into the processes and mechanisms involved with these future connections, and that is the goal of the present paper.

Many previous studies have analyzed multi-model ensembles and have identified a large model dependence regarding future South Asian monsoon characteristics (Annamalai et al., 2007; Jayasankar et al., 2015;

Resources: Aixue Hu, Jean-Christophe Golaz, Luke Van Roekel
Software: Christine A. Shields, Julie M. Arblaster, John Fasullo, Nan Rosenbloom, Aixue Hu, Jean-Christophe Golaz, Luke Van Roekel
Supervision: Gerald A. Meehl
Validation: Christine A. Shields, Nan Rosenbloom, Richard Neale, Jean-Christophe Golaz, Luke Van Roekel, H. Annamalai
Visualization: John Fasullo
Writing – original draft: Gerald A. Meehl
Writing – review & editing: Gerald A. Meehl, Christine A. Shields, Julie M. Arblaster, Antonietta Capotondi

Katzenberger et al., 2021; Li & Ting, 2015; Turner et al., 2007). Therefore, this paper addresses the model-dependence issue by analyzing large ensembles of two related Earth system models in detail to identify physical processes that contribute to different future South Asian monsoon outcomes. The eventual goal is to increase understanding of the processes and mechanisms that could contribute to seasonal to decadal prediction skill. We hypothesize that increased ENSO amplitude can strengthen future monsoon-ENSO connections, and/or that the magnitude and pattern of warming in the tropical eastern Pacific can affect the strength and zonal displacement of the Walker circulation that could affect how strongly the Pacific connects to the South Asian monsoon.

Here we perform a "two model analysis" (e.g., Baumhefner, 1976; Meehl et al., 2023) using E3SMv2 and CESM2 to analyze how the simulation of key processes can produce different outcomes for future mean monsoon precipitation and monsoon-ENSO connections. The rationale and utility of such two model analyses are discussed in Meehl et al. (2023) where a comparable two model analysis was performed to study present-day monsoon processes. In summary, a single model analysis is just that: results from a single model with no indication of how to generalize the results. An alternative is an analysis of CMIP models with more samples, but with no insight into what about the models is producing the results. A two-model analysis allows detailed study of processes in the context of a familiarity with simulation characteristics in the two models. Such analyses provide the framework for understanding the relevant physical mechanisms that could inform more detailed studies of monsoon projections from the full suite of CMIP6 models.

2. Models

The CESM2 is fully described by Danabasoglu et al. (2020), and its responses to increasing greenhouse gasses in a future warmer climate are provided by Meehl et al. (2020). The atmospheric and ocean models in CESM2 have a nominal 1-degree latitude-longitude resolution. The ocean model in CESM2 is a version of POP2 (Parallel Ocean Program, version 2) with 1-degree latitude-longitude resolution, enhanced resolution in the equatorial tropics, and 60 levels in the vertical with ocean biogeochemistry.

The E3SMv2 also has a nominal 1° resolution (110-km atmosphere, 165-km land, 0.5° river model), while the ocean and sea ice have a mesh spacing varying between 60 km in the mid-latitudes and 30 km at the equator and poles (fully described by Golaz et al. (2022); some characteristics of future monsoon changes are described by Harrop et al. (2019)). The ocean represents the biggest physical difference between E3SMv2 and CESM2. The latter includes a conventional grid point ocean model, POP2, and the former uses MPAS-Ocean with a different grid and other structural differences noted in Supporting Information S1 and in Petersen et al. (2019). Meehl et al. (2023) contrasted monsoon and monsoon-ENSO features in the two models for present-day climate. For context here (and also discussed in various places to follow), the patterns of simulated South Asian monsoon precipitation are similar between the two models for present-day climate, but present-day monsoon-ENSO teleconnections through the Walker Circulation are weaker in E3SMv2 compared to CESM2 due to cooler mean tropical SSTs, along with ENSO amplitude in E3SMv2 that is half that in CESM2.

Aerosols have been recognized as playing a part in producing certain monsoon characteristics (Bollasina et al., 2011; Meehl et al., 2008; Persad et al., 2023). However, the effects of different aerosol forcings in the two models, which are difficult to quantify, are beyond the scope of the present paper.

A factor for comparing future climate change in the two models is that equilibrium climate sensitivity (ECS) is greater in CESM2 compared to E3SMv2, with an ECS of about 5.2°C in CESM2 (Danagasoglu et al., 2020) and 4.0°C in E3SMv2 (Golaz et al., 2022). Thus, the starting point for understanding relative differences in monsoon characteristics is the future warming of tropical SSTs as discussed below.

Model simulations for CESM2 and E3SMv2 include 20 ensemble members each and are run for future climate with the SSP370 emission scenario from 2015 to 2100. Note that there are more ensemble members available from the CESM2 large ensemble, but we choose to use 20 of them to match the 20 ensemble members available from E3SMv2. Including more ensemble members does not change the conclusions. Seasonal mean changes are computed for the June-July-August-September (JJAS) monsoon season. A fuller description of the two models is given in the Supporting Information S1.

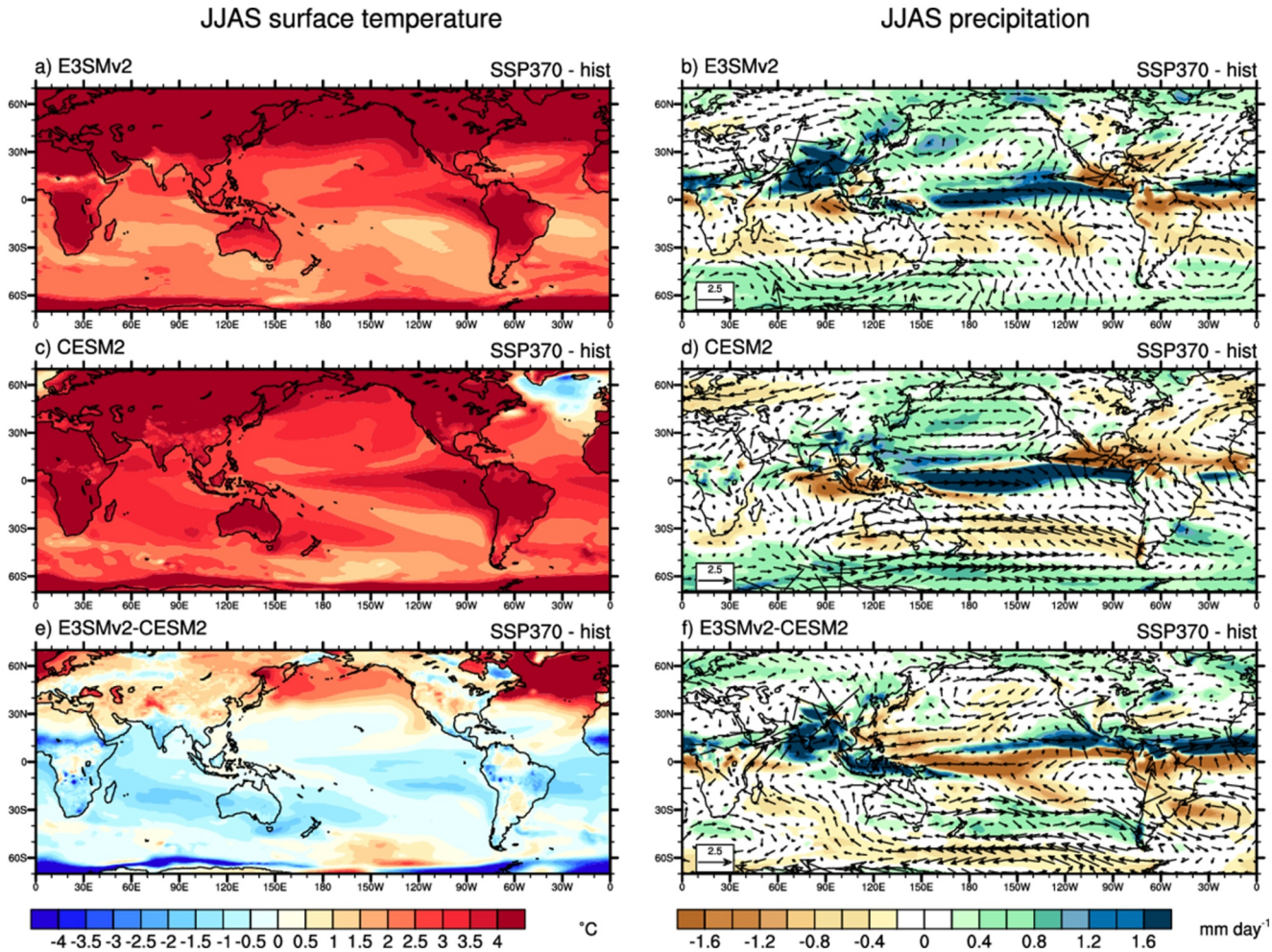

Figure 1. Future (2081–2100) minus historical (1995–2014), JJAS, for (a) E3SMv2 surface temperature (°C); Panel (b) same as panel (a) except for precipitation (mm day^{-1}), colors, and 850 hPa wind vectors (m sec^{-1}), scaling arrow at lower left; Panel (c) same as panel (a) except for CESM2; Panel (d) same as panel (b) except for CESM2; (e) Difference (a) minus (c); Panel (f) same as panel (e) except for difference (b) minus (d). Differences generally greater in magnitude than +/−0.5°C for temperature and +/−0.2 mm day^{-1} for precipitation are significant at the 95% level.

3. Future South Asian Monsoon Season Mean Changes

On average, the E3SMv2 has somewhat less future warming in the tropics compared to CESM2 (Figures 1a and 1c) with negative SST differences for E3SMv2 minus CESM2 of over −1°C in some parts of the tropical Indian and Pacific Oceans (Figure 1e). Averaged over the tropical Pacific (80°W–150°E, 15°N–15°S) for the future (2081–2100) minus present (1995–2014) time periods, CESM2 warms by 3.0°C (standard deviation 0.08°C), while E3SMv2 warms by 2.7°C (standard deviation 0.08°C) (Figure 2a), with comparable increases over the tropical Indian Ocean (Figure 1e).

However, there are more marked differences in the future south Asian monsoon precipitation between the two models. Figure 1f shows that E3SMv2 clearly has a larger increase in future south Asian monsoon precipitation compared to CESM2. Averaged over all grid points in the south Asian monsoon domain (5°N–40°N, 60°E–100°E), E3SMv2 has a future minus present increase of monsoon precipitation of +1.37 mm day^{-1} (standard deviation of 0.15 mm day^{-1}) or about 24%, compared to the increase in CESM2 of only +0.22 mm day^{-1} or roughly 5% (standard deviation of 0.12 mm day^{-1}) (Figure 2a). This is an interesting result since it might be expected that the monsoon precipitation increase in E3SMv2 would be less than in CESM2 since the tropical Indian Ocean warms nearly 1°C less in E3SMv2 compared to CESM2 (Figure 1e) with an implied relatively reduced source of moisture to be advected into southern Asia to fuel monsoon precipitation (Rajendran

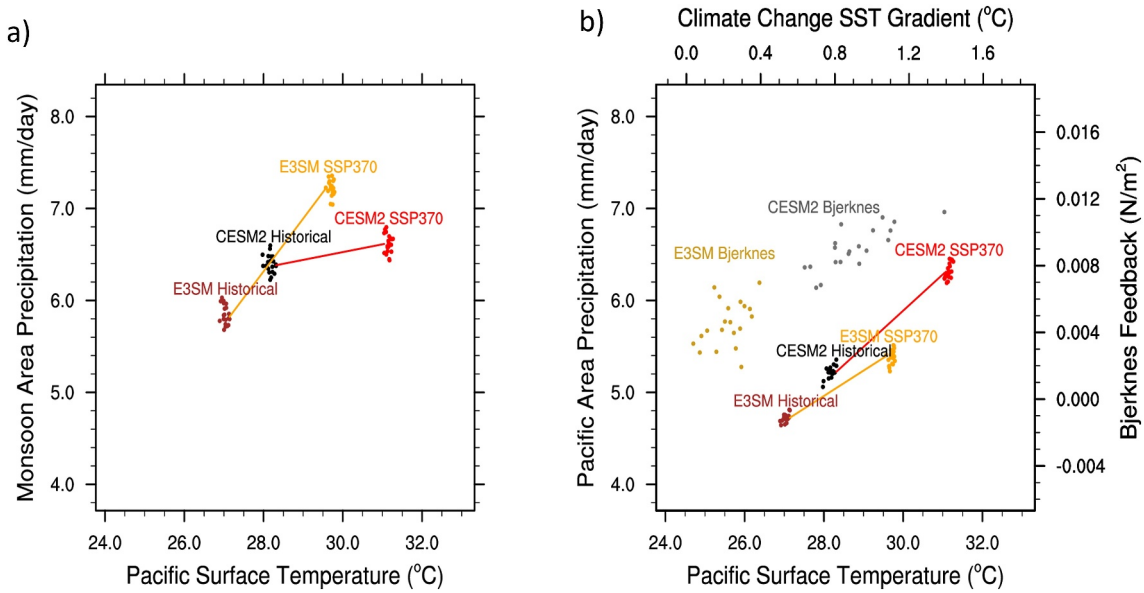

Figure 2. (a) South Asian monsoon area-averaged precipitation, JJAS (mm day^{-1}), averaged over all grid points 5°N–40°N, 60°E–100°E on *y* axis as a function of tropical Pacific average SSTs (°C) averaged over 80°W–150°E, 15°N–15°S on the *x* axis, for historical and future climate averages as in Figure 1, for E3SMv2 and CESM2; dots indicate values from individual ensemble members, solid line connects ensemble mean for present-day climate to future climate; (b) for values in lower part of panel, *y* axis on left denotes tropical Pacific area-averaged precipitation (mm day^{-1}), for all grid points averaged over 80°W–150°E, 15°N–15°S plotted as a function of tropical Pacific average SSTs (°C) averaged over 80°W–150°E, 15°N–15°S on the *x* axis at bottom, for historical and future climate averages as in Figure 1, for E3SMv2 and CESM2; dots indicate values from individual ensemble members, solid line connects ensemble mean for present-day climate to future climate; dots for individual ensemble members labeled "E3SM Bjerknes" and "CESM2 Bjerknes" plotted for the future minus present change in SST gradient defined over the eastern equatorial Pacific Niño3.4 area (5°N–5°S and 170°–120°W) minus a western tropical Pacific region (5°S–5°N and 120°E–160°E), values related to *x* axis label at top, plotted as a function of Bjerknes feedback on *y* axis on right defined as the average of u component surface wind stress anomalies, future minus present, averaged spatially across the entire equatorial Pacific basin (170°E–90°W; 5°S–5°N).

et al., 2022). Yet, as noted above there is about a factor of 7 larger relative increase of monsoon precipitation in E3SMv2 (+1.37 mm day^{-1}) compared to CESM2 (+0.22 mm day^{-1}) (Figures 1f and 2a).

Clearly there are other factors influencing future monsoon precipitation in the two models, since previous studies have identified warmer Indian Ocean SSTs that can produce greater monsoon precipitation, along with the effects of enhanced meridional temperature gradient and forcing through the Walker Circulation from the tropical Pacific (Meehl & Arblaster, 2002). This suggests that contrasting changes in simulated circulations may be responsible for the difference (e.g., Li et al., 2015). Previous research has suggested that the large-scale zonal tropical circulation (the Walker Circulation), which connects precipitation in the Indian and Pacific sectors, is likely to be involved (e.g., Meehl, 1987; Rasmusson & Carpenter, 1983). The future precipitation change in E3SMv2 shows that the greatest decreases in tropical Pacific precipitation are shifted a bit south and extend across the equatorial Pacific to South America compared to CESM2 (Figures 1b–1d and 1f). While both models show an El Niño-like response (greater warming in the eastern tropical Pacific than the west), this response is larger in CESM2 (Figures 1a and 1c). This can be quantified by computing the eastern tropical Pacific minus western tropical Pacific SST differences. This east-west SST gradient is defined here as the change of the SST difference for an eastern Pacific region defined over the Niño3.4 area (5°N–5°S and 170°–120°W) minus a western Pacific region (5°S–5°N and 120°E–160°E). For E3SMv2, the average change, future minus present, is 0.22 + / − 0.10°C (range for this and other values is +/− one standard deviation across the ensemble members), and for CESM2 it is over four times larger with a value of 0.92 + / − 0.18°C (Figure 2b). The magnitude of the El Niño-like response is directly related to the Bjerknes feedback (Fu & Fedorov, 2023). This is defined here as the zonal component of surface wind stress anomalies averaged spatially across the entire equatorial Pacific basin (170°E–90°W; 5°S–5°N). For CESM2 this average change is +0.009 + / − 0.001 N/m^2, and for E3SMv2 it is less than half that with a value of +0.004 +/− 0.001 N/m^2 (Figure 2b). The amplifying effects of moisture convergence in the Western Pacific Ocean associated with the greater increase in the zonal moist static energy (MSE) gradient is likely to further amplify the Walker Circulation response under climate change in CESM2 versus E3SMV2 (Figure S1 in Supporting Information S1). The stronger Bjerknes feedback in CESM2 means that stronger westerly surface

wind stress anomalies would weaken upwelling and provide a feedback to increase SST anomalies in the eastern Pacific compared to the west (e.g., Zheng et al., 2014). Thus, the CESM2, with its larger Bjerknes feedback and associated processes that amplify warming, has a consequent greater El Niño-like response (larger amplitude east minus west SST anomalies) (Figure 2b). The relationship between SST and precipitation over the Pacific (e.g., Yun et al., 2021) is illustrated in Figure 2b. The CESM2, with warmer present-day base state SSTs of about 1°C compared to E3SMv2, has a larger increase in tropical Pacific SSTs in future climate of 3.00°C +/− 0.08°C (to go along with the larger El Niño-like response) and an increase of tropical Pacific precipitation of about 22% (1.10 mm day^{-1} +/− 0.11 mm day^{-1}). This can be compared to E3SMv2 that has less of a future increase in tropical Pacific SSTs of 2.68°C +/− 0.08°C (to go along with the smaller El Niño-like response) and a smaller amplitude increase in Pacific precipitation of about 14% (0.66 mm day^{-1} +/− 0.08 mm day^{-1}) (Figure 2b).

Therefore, along with higher climate sensitivity, warmer base state present-day tropical SSTs in CESM2 contribute to relatively warmer future SSTs over the tropical Pacific compared to E3SMv2 due in part to a stronger Bjerknes feedback that amplifies eastern Pacific SST anomalies. That is, even if the climate change warming of tropical Pacific SSTs was the same in E3SMv2 and CESM2, the warmer starting point of present-day SSTs in CESM2 would mean proportionately greater precipitation over the eastern equatorial Pacific in the future compared to E3SMv2 due to the nonlinear relationship between surface warming and consequent precipitation (e.g., Trenberth et al., 2003). Greater precipitation over the eastern equatorial Pacific results in larger anomalous westerly wind stress and thus in a larger positive Bjerknes feedback that would contribute to amplifying the warming of eastern tropical Pacific SSTs (Figure 2b) and produce proportionately greater precipitation in CESM2 compared to E3SMv2. A consequence of a relatively larger increase of precipitation over the Pacific in CESM2 compared to E3SMv2 is a relatively smaller increase of future South Asian monsoon precipitation in CESM2 (Figure 2a). This occurs through the anomalous Walker Circulation that we turn to next.

Changes in the Walker Circulation are often represented by differences in the 200 hPa velocity potential (e.g., Meehl & Arblaster, 2011). In Figure S2 in Supporting Information S1, we show JJAS season differences for mean Walker Circulation changes to correspond to the mean season changes in monsoon precipitation in Figure 1. There are significant positive differences of $+2 \times 10^6$ m^2 sec^{-2} of 200 hPa velocity potential over the tropical Pacific for E3SMv2 minus CESM2 indicating relative increases in upper-level convergence there in E3SMv2. Meanwhile, there are significant negative 200 hPa velocity potential differences of about -4×10^6 m^2 sec^{-2} over the South Asian monsoon region in Figure S2a in Supporting Information S1 for E3SMv2 minus CESM2 indicating relatively stronger upper-level divergence in E3SMv2. This is associated with stronger upward vertical motion (blue colors in Figure S2b in Supporting Information S1) associated with the larger increases in monsoon precipitation in E3SMv2 (Figure 2a). Positive differences in 200 hPa velocity potential for E3SMv2 minus CESM2 (Figure S2a in Supporting Information S1) indicate relatively greater downward vertical motion over the tropical Pacific (orange colors in Figure S2b in Supporting Information S1) where the precipitation increases are less in E3SMv2 compared to CESM2 (Figure 2b). Therefore, these dynamical processes involving the Walker Circulation represent the mechanisms involved with the relatively larger increases of future South Asian monsoon precipitation in E3SMv2 compared to CESM2.

Another factor contributing to the relative enhancement of monsoon precipitation in E3SMv2 compared to CESM2 is the greater future warming over the Tibetan Plateau region of South Asia in E3SMv2 that produces an enhanced meridional temperature gradient which, as noted earlier, can affect monsoon precipitation. An enhanced meridional temperature gradient between the Tibetan Plateau and areas over southern India and the Indian Ocean is a well-known contributor to stronger monsoon precipitation (e.g., Blanford, 1884; Li & Yanai, 1996; Meehl, 1994; Meehl & Arblaster, 2002), and is another element that contributes to enhancing future monsoon precipitation in E3SMv2 compared to CESM2. The difference of surface temperature anomalies (Figure 1e) averaged between 70°E−90°E for 45°N minus 20°N (Meehl & Arblaster, 2002) produces an enhanced meridional temperature gradient in the MAM season of +1.6°C. This sets the stage for a subsequent stronger monsoon and an enhanced meridional temperature gradient with a difference of +2.4°C. The greater precipitation during the monsoon season of JJAS contributes to relatively cooler surface temperatures over the Indian subcontinent due to increased cloudiness, reduced incoming solar radiation, and enhanced latent heat flux (e.g., Meehl & Arblaster, 2002). Figure 1f shows that E3SMv2 clearly has a larger increase in future south Asian monsoon precipitation compared to CESM2, and this is consistent with energetic constraints arising from a greater increase in boundary layer MSE (Figure S1 in Supporting Information S1; Biasutti et al., 2018).

4. Future Monsoon-ENSO Connections

Previous studies have shown evidence that a future warmer base state and/or future increased ENSO amplitude contribute to stronger monsoon-ENSO connections (e.g., Meehl et al., 2023). The warmer base state tropical SSTs and larger amplitude ENSO in CESM2 (Capotondi et al., 2020) produce a stronger monsoon-ENSO connection in present-day climate, with each contributing about half to the total change (Meehl et al., 2023). Consequently, in the future warmer climate state in both models, the monsoon-ENSO connections are stronger as derived from the average of time series correlations of All-India Rainfall (AIR) with Niño3.4 SSTs in the two models (Figure S3 in Supporting Information S1). The negative correlation between Niño3.4 SSTs and AIR (indicating that when SSTs are anomalously warm in the eastern equatorial Pacific there tends to be reduced monsoon precipitation) increases from an average of −0.63 to −0.68 (around 8%) in CESM2, and from roughly −0.41 to −0.54 (about 32%) in E3SMv2 (Figure S3 in Supporting Information S1). This result can be partly attributed to future changes of ENSO amplitude (Figure S4 in Supporting Information S1) where E3SMv2 has increases of ENSO amplitude of about 36% (measured by largest amplitude spectra), while CESM2 ENSO amplitude actually decreases slightly by roughly −9% for this specific time interval of 2040–2100, with the caveat that changes in amplitude are temporally complex due to internal decadal variability (Meehl et al., 2023). Thus, one of the two main contributors to the strength of the monsoon-ENSO connection in present-day climate documented by Meehl et al. (2023), ENSO amplitude, is a contributor to the future relative strengthening of the monsoon-ENSO connection in E3SMv2. Additionally, there is higher ENSO frequency in both models with maximum values near 0.03 cycles mo^{-1}, while observations are closer to 0.02 cycles mo^{-1}. Since both models have this same characteristic, we assume this does not play a role in the relative changes in the monsoon-ENSO connection, though research to quantify the effects of different ENSO frequencies on the monsoon-ENSO connection are beyond the scope of this paper.

Another factor that produces a relative strengthening of the monsoon-ENSO relationship in E3SMv2 compared to CESM2 is illustrated by the associated dynamical connections. Figure 3 shows the changes, future minus historical, of the regression of Niño3.4 SSTs onto 200 hPa velocity potential. Both E3SMv2 (Figure 3a) and CESM2 (Figure 3b) show negative values over the tropical Pacific and positive values over the western Pacific region, indicative of the well-known Walker Circulation connections between Australasia and the central/eastern tropical Pacific (e.g., see Meehl et al., 2023 for present-day climate in these two models). However, this pattern is shifted eastward in CESM2 (Figure 3b) compared to E3SMv2 (Figure 3a). This moves the Walker Circulation centers of action away from the monsoon region, thus weakening that connection in CESM2 compared to E3SMv2, relatively speaking. A reason for this shift can be seen in the mean change of the Pacific center of action of the Walker Circulation in E3SMv2 compared to CESM (Figure S2a in Supporting Information S1). There are significant positive differences greater than $+2 \times 10^6$ m^2 sec^{-2}, indicating enhanced upper level convergence there in E3SMv2. As this is a region of top-heavy deep convection, the enhanced response of upper-level divergence in E3SMv2 is consistent with energetic constraints tied to MSE, as shown in Figure 1 and Figure S1 in Supporting Information S1, where greater increases are associated with enhanced upper level divergence (Biasutti et al., 2018). These extend across the eastern tropical Pacific south of the equator and over tropical South America, and roughly correspond to many areas of significant negative precipitation differences in Figure 1f. This indicates an eastward shift in CESM2, compared to E3SMv2, of the Walker Circulation centers of action associated with the stronger El Niño-like response (Figure 2b) and relatively warmer eastern tropical Pacific SSTs in CESM2. This has previously been shown to reduce monsoon-ENSO connections for the Australian monsoon (e.g., Arblaster et al., 2002) as well as the south Asian monsoon (Meehl & Arblaster, 2011). There is an enhanced meridional temperature gradient in future climate in E3SMv2 compared to E3SM2 between the Tibetan Plateau and southern India that was noted earlier. Previous work has indicated that forcing from the tropical Pacific likely plays a larger role than enhanced meridional temperature gradient in future monsoon changes (e.g., Meehl & Arblaster, 2002), though this research topic deserves further study that is beyond the scope of the present paper.

5. Broader Implications

It is desirable to attempt to relate the processes identified in the two models analyzed here to the CMIP6 models. However, analysis of CMIP5 and CMIP6 models indicates that significant additional structural uncertainties among the models affect the simulation of the south Asian monsoon (Singh et al., 2019), and many models fail to adequately simulate observed ENSO characteristics (Wang et al., 2023) or monsoon-ENSO connections (e.g., Li & Ting, 2015; Lin et al., 2023). These confounding biases make attempts to generalize monsoon-ENSO related

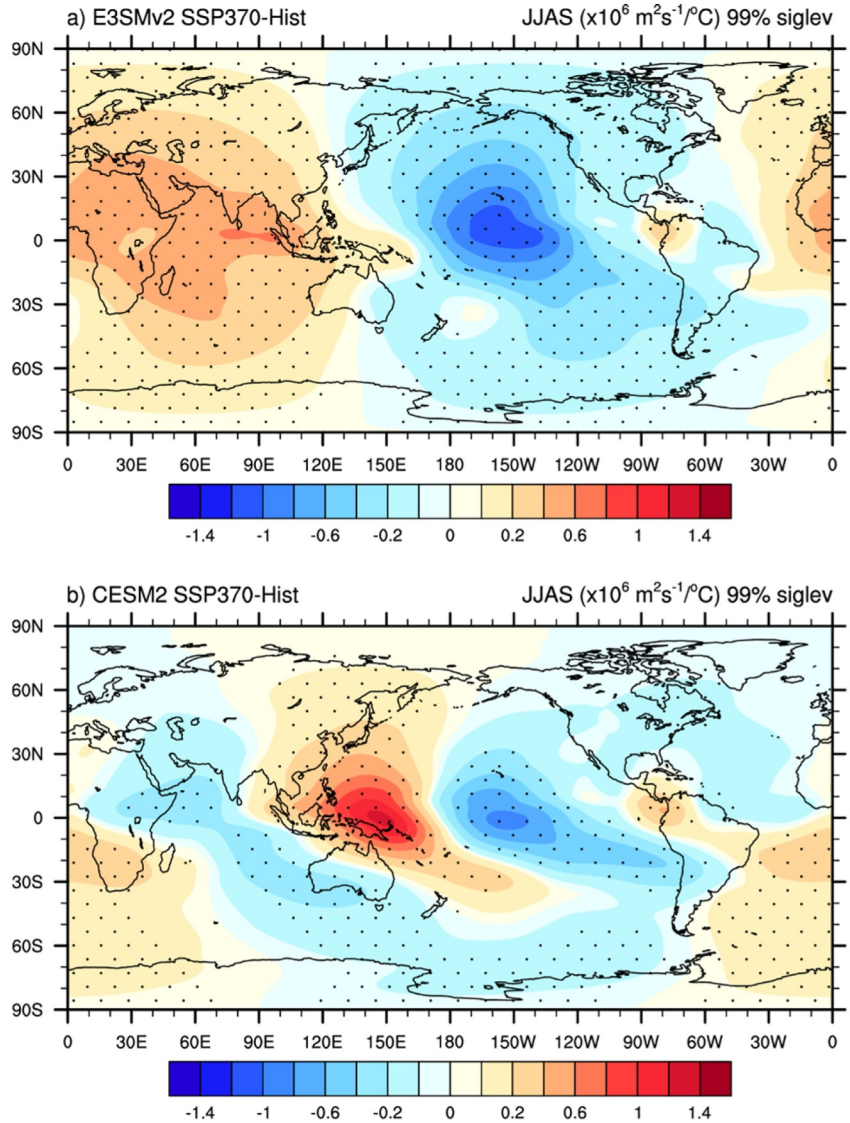

Figure 3. Differences, future minus historical, in the regression coefficients for each time period computed separately for the Niño3.4 time series regressed onto 200 hPa velocity potential, JJAS (x 10^6 m^2 sec^{-2}/°C), for (a) E3SMv2, (b) CESM2; stippling indicates 99% significance.

processes in a future warmer climate across the strikingly disparate set of CMIP6 models not meaningful. Additionally, many CMIP6 models (of which E3SMv2 and CESM2 are members) have difficulty simulating climatic features relevant to monsoon-ENSO interactions (Rajendran et al., 2022) arising from biases in the eastern Pacific cold tongue and base state SSTs in the tropical Pacific and elsewhere in present (Wang et al., 2020) and future climate (Xiang et al., 2014). These features result in substantial differences in the consistency of ENSO across the models and complicate the interpretation of inter-model contrasts for future changes in monsoon precipitation and monsoon-ENSO connections in the models (Meehl et al., 2023). Correcting the various biases that differ across the models, so that the effects of their simulation characteristics can be used in a consistent enough way to attempt to generalize the processes discussed here, is beyond the scope of the present paper. However, this represents an important research priority for the climate science community. That the two present models have similar monsoon simulation characteristics and ENSO features, and less structural uncertainty compared to other CMIP6 models (Meehl et al., 2023), makes the present interpretation of processes and mechanisms of possible future South Asian monsoon behavior related to monsoon-ENSO connections more credible and physically feasible. This points to the value of a comparable future study with a more consistent

multi-model subset. However, the key processes we have identified in the present study, with regards to their important effects on future monsoon-ENSO connections, are ENSO amplitude and the size of the future El Niño-like response in tropical Pacific SSTs.

Data Availability Statement

All-India Rainfall data is available from Indian Institute of Tropical Meteorology (2024). E3SM model code is available at E3SM Project (2024). E3SM model data is available at E3SM Project (2023). CESM model code is available at CESM Project (2024). CESM model data is available at CESM Project (2023).

Acknowledgments
Portions of this study were supported by the Regional and Global Model Analysis (RGMA) component of the Earth and Environmental System Modeling Program of the U.S. Department of Energy's Office of Biological & Environmental Research (BER) under Award Number DE-SC0022070. This work also was supported by the National Center for Atmospheric Research, which is a major facility sponsored by the National Science Foundation (NSF) under Cooperative Agreement No. 1852977. The Energy Exascale Earth System Model (E3SM) project is funded by the U.S. Department of Energy, Office of Science, Office of Biological and Environmental Research (BER). E3SM simulations were performed at the National Energy Research Scientific Computing Center (NERSC), a DOE Office of Science User Facility supported by the Office of Science of the U.S. Department of Energy under Contract No. DE-AC02-05CH11231. The CESM project is supported primarily by the NSF. Computing and data storage resources, including the Cheyenne supercomputer, were used for the CESM simulations (doi:10.5065/D6RX99HX). H. Annamalai is supported by an NSF project under Grant 1460742. A. Capotondi was supported by DOE Award #DE-SC0023228. Lawrence Livermore National Laboratory is operated by Lawrence Livermore National Security, LLC, for the U.S. Department of Energy, National Nuclear Security Administration under Contract DE-AC52-07NA27344.

References

Annamalai, H., Hamilton, K., & Sperber, K. R. (2007). South Asian summer monsoon and its relationship with ENSO in the IPCC AR4 simulations. *Journal of Climate*, *20*(6), 1071–1092. https://doi.org/10.1175/jcli4035.1

Arblaster, J. M., Meehl, G. A., & Moore, A. (2002). Interdecadal modulation of Australian rainfall. *Climate Dynamics*, *18*(6), 519–531. https://doi.org/10.1007/s00382-001-0191-y

Ashfaq, M., Shi, Y., Tung, W., Trapp, R. J., Gao, X., Pal, J. S., & Diffenbaugh, N. S. (2009). Suppression of south Asian summer monsoon precipitation in the 21st century. *Geophysical Research Letters*, *36*(1). https://doi.org/10.1029/2008GL036500

Baumhefner, D. (1976). A single forecast comparison between the NCAR and GFDL general circulation models. *Monthly Weather Review*, *104*(9), 1175–1177. https://doi.org/10.1175/1520-0493(1976)104<1175:ASFCBT>2.0.CO;2

Beljaars, A. C. M., Brown, A. R., & Wood, N. (2004). A new parametrization of turbulent orographic form drag. *Meteorol. Soc.*, *130*(599), 1327–1347. https://doi.org/10.1256/qj.o3.73

Biasutti, M., Voigt, A., Boos, W. R., Braconnot, P., Hargreaves, J. C., Harrison, S. P., et al. (2018). Global energetics and local physics as drivers of past, present and future monsoons. *Nature Geoscience*, *11*(6), 392–400. https://doi.org/10.1038/s41561-018-0137-1

Blanford, H. F. (1884). On the connexion of Himalayan snowfall and seasons of drought in India. In *Proc. Roy. Soc.* (pp. 3–22).

Bollasina, M. A., Yi Ming, Y., & Ramaswamy, V. (2011). Anthropogenic aerosols and the weakening of the South Asian summer monsoon. *Science*, *334*(6055), 502–505. https://doi.org/10.1126/science.1204994

Bonfils, C. J. W., Santer, B. D., Phillips, T. J., Marvel, K., Leung, L. R., Doutriaux, C., & Capotondi, A. (2015). Relative contributions of mean-state shifts and ENSO-driven variability to precipitation changes in a warming climate. *Journal of Climate*, *28*(24), 9997–10013. https://doi.org/10.1175/JCLI-D-15-0341.1

Bradley, A. M., Bosler, P. A., & Guba, O. (2021). Islet: Interpolation semi-lagrangian element-based transport. *Geoscientific Model Development Discussions*, 1–48. https://doi.org/10.5194/gmd-2021-296

Cai, W., Ng, B., Wang, G., Santoso, A., Wu, L., & Yang, K. (2022). Increased ENSO sea surface temperature variability under four IPCC emission scenarios. *Nature Climate Change*, *12*(3), 228–231. https://doi.org/10.1038/s41558-022-01282-z

Capotondi, A., et al. (2020). *ENSO and Pacific decadal variability in CESM2*. JAMES. https://doi.org/10.1029/2019MS002022

CESM Project. (2023). Community Earth System Model (CESM) version 2 monthly mean data from the CESM2 large ensemble (LENS), reformatted following CMIP conventions [Dataset]. https://www.cesm.ucar.edu/community-projects/lens2/data-sets

CESM Project. (2024). Community Earth System Model (CESM), April 2, 2020 release (version 2.1.3) [Software]. https://github.com/ESCOMP/CESM

Choudhury, D., Nath, D., & Chen, W. (2022). Near future projection of Indian summer monsoon circulation under 1.5°C and 2.0°C warming. *Atmosphere*, *13*(7), 1081. https://doi.org/10.3390/atmos13071081

Danabasoglu, G., Lamarque, J., Bacmeister, J., Bailey, D. A., DuVivier, A. K., Edwards, J., et al. (2020). *The Community Earth System Model version 2 (CESM2)*, JAMES, (Vol. 12), e2019MS001916. https://doi.org/10.1029/2019MS001916

Douville, H., Royer, J.-F., Polcher, J., Cox, P., Gedney, N., Stephenson, D. B., & Valdes, P. J. (2000). Impact of CO_2 doubling on the Asian summer monsoon: Robust versus model-dependent responses. *Journal of the Meteorological Society of Japan*, *78*(4), 421–439. https://doi.org/10.2151/jmsj1965.78.4_421

E3SM Project. (2023). Energy Exascale Earth System Model version 2 monthly mean data reformatted following CMIP conventions [dataset]. *DOE Earth System Grid Federation (ESGF)*. https://esgf-node.llnl.gov/projects/e3sm

E3SM Project. (2024). Energy Exascale Earth System Model (E3SM), October 11, 2021 release (version 2.0) [Software]. https://doi.org/10.11578/E3SM/dc.20240301.3

Fu, M., & Fedorov, A. (2023). The role of Bjerknes and shortwave feedbacks in the tropical Pacific SST response to global warming. *Geophysical Research Letters*, *50*(19), e2023GL105061. https://doi.org/10.1029/2023GL105061

Gettelman, A., & Morrison, H. (2015). Advanced two-moment bulk microphysics for global models. Part I: Off-line tests and comparison with other schemes. *Journal of Climate*, *28*(3), 1268–1287. https://doi.org/10.1175/JCLI-D-14-00102.1

Gnanadesikan, A., Russell, A., Pradal, M.-A., & Abernathey, R. (2017). Impact of lateral mixing in the ocean on El Niño in a suite of fully coupled climate models. *Journal of Advances in Modeling Earth Systems*, *9*(7), 2493–2513. https://doi.org/10.1002/2017MS000917

Golaz, J.-C., Caldwell, P. M., Van Roekel, L. P., Petersen, M. R., Tang, Q., Wolfe, J. D., et al. (2019). The DOE E3SM coupled model version 1: Overview and evaluation at standard resolution. *Journal of Advances in Modeling Earth Systems*, *11*(7), 2089–2129. https://doi.org/10.1029/2018ms001603

Golaz, J.-C., Van Roekel, L. P., Zheng, X., Roberts, A. F., Wolfe, J. D., Lin, W., et al. (2022). The DOE E3SM model version 2: Overview of the physical model. *Journal of Advances in Modeling Earth Systems*, *14*(12), e2022MS003156. https://doi.org/10.1029/2022MS003156

Goswami, B. B., & An, S.-I. (2023). An assessment of the ENSO-monsoon teleconnection in a warming climate. *npj Climate and Atmospheric Science*, *6*(1), 82. https://doi.org/10.1038/s41612-023-00411-5

Harrop, B. E., Ma, P.-L., Rasch, P. J., Neale, R. B., & Hannay, C. (2018). The role of convective gustiness in reducing seasonal precipitation biases in the tropical West Pacific. *Journal of Advances in Modeling Earth Systems*, *1*(4), 1–10. https://doi.org/10.1002/2017MS001157

Harrop, B. E., Ma, P.-L., Rasch, P. J., Qian, Y., Lin, G., & Hannay, C. (2019). Understanding monsoonal water cycle changes in a warmer climate in E3SMv1 using a normalized gross moist stability framework. *Journal of Geophysical Research: Atmospheres*, *124*(20), 10–826. https://doi.org/10.1029/2019JD031443

Hurrell, J. W., Holland, M. M., Gent, P. R., Ghan, S., Kay, J. E., Kushner, P. J., et al. (2013). The Community Earth System Model: A framework for collaborative research. *Bulletin America Meteorology Social*, *94*(9), 1339–1360. https://doi.org/10.1175/bams-d-12-00121.1

Indian Institute of Tropical Meteorology. (2024). All-India rainfall index [Dataset]. https://www.tropmet.res.in/data/data-archival/rain/iitm-regionrf.txt

Jayasankar, C. B., Surendran, S., & Rajendran, K. (2015). Robust signals of future projections of Indian summer monsoon rainfall by IPCC AR5 climate models: Role of seasonal cycle and interannual variability. *Geophysical Research Letters*, *42*(9), 3513–3520. https://doi.org/10.1002/2015GL063659

Jin, Q., & Wang, C. (2017). A revival of Indian summer monsoon rainfall since 2002. *Nature Climate Change*, *7*(8), 587–594. https://doi.org/10.1038/nclimate3348

Kamae, Y., Watanabe, M., Kimoto, M., & Shiogama, H. (2014). Summer-time land-sea thermal contrast and atmospheric circulation over East Asia in a warming climate—Part II: Importance of CO_2-induced continental warming. *Climate Dynamics*, *43*(9–10), 2569–2583. https://doi.org/10.1007/s00382-014-2146-0

Katzenberger, A., Schewe, J., Pongratz, J., & Levermann, A. (2021). Robust increase of Indian monsoon rainfall and its variability under future warming in CMIP6 models. *Earth System Dynamics*, *12*(2), 367–386. https://doi.org/10.5194/esd-12-367-2021

Kripalani, R. H., Oh, J. H., Kulkarni, A., Sabade, S. S., & Chaudhari, H. S. (2007). South Asian summer monsoon precipitation variability: Coupled climate model simulations and projections under IPCC AR4. *Theoretical and Applied Climatology*, *90*(3–4), 133–159. https://doi.org/10.1007/s00704-006-0282-0

Larson, V. E. (2017). *CLUBB-SILHS: A parameterization of subgrid variability in the atmosphere*, arXiv, (Vol. 1711), 03675v4. https://doi.org/10.48550/ARXIV.1711.03675

Li, C., & Yanai, M. (1996). The onset and interannual variability of the Asian summer monsoon in relation to land-sea thermal contrast. *Journal of Climate*, *9*(2), 358–375. https://doi.org/10.1175/1520-0442(1996)009<0358:toaivo>2.0.co;2

Li, X., & Ting, M. (2015). Recent and future changes in the Asian monsoon-ENSO relationship: Natural or forced? *Geophysical Research Letters*, *42*(9), 3502–3512. https://doi.org/10.1002/2015GL063557

Li, X., & Ting, M. (2017). Understanding the asian summer monsoon response to greenhouse warming: The relative roles of direct radiative forcing and sea surface temperature change. *Climate Dynamics*, *49*(7–8), 2863–2880m. https://doi.org/10.1007/s00382-016-3470-3

Li, X., Ting, M., Li, C., & Henderson, N. (2015). Mechanisms of Asian summer monsoon changes in response to anthropogenic forcing in CMIP5 models. *Journal of Climate*, *28*(10), 4107–4125. https://doi.org/10.1175/JCLI-D-14-00559.1

Lin, S., Buwen, D., Yang, S., Shan, H., & Hu, Y. (2023). Causes of diverse impacts of ENSO on the Southeast Asian summer monsoon among CMIP6 models. *Journal of Climate*. https://doi.org/10.1175/JCLI-D-23-0303.1

Liu, X., Ma, P.-L., Wang, H., Tilmes, S., Singh, B., Easter, R. C., et al. (2016). Description and evaluation of a new four-mode version of the Modal Aerosol Module (MAM4) within version 5.3 of the community atmosphere model. *Geoscientific Model Development*, *9*(2), 505–522. https://doi.org/10.5194/gmd-9-505-2016

Ma, P.-L., Harrop, B. E., Larson, V. E., Neale, R. B., Gettelman, A., Morrison, H., et al. (2022). Better calibration of cloud parameterizations and subgrid effects increases the fidelity of E3SM Atmosphere Model version 1. *Geoscientific Model Development*, *15*(7), 2881–2916. https://doi.org/10.5194/gmd-15-2881-2022

McGregor, S., Cassou, C., Kosaka, Y., & Phillips, A. S. (2022). Projected ENSO teleconnection changes in CMIP6. *Geophysical Research Letters*, *49*(11), e2021GL097511. https://doi.org/10.1029/2021GL097511

Meehl, G. A. (1987). The annual cycle and interannual variability in the tropical Pacific and Indian Ocean regions. *Monthly Weather Review*, *115*(1), 27–50. https://doi.org/10.1175/1520-0493(1987)115<0027:tacaiv>2.0.co;2

Meehl, G. A. (1994). Coupled land-ocean-atmosphere processes and south Asian monsoon variability. *Science*, *266*(5183), 263–267. https://doi.org/10.1126/science.266.5183.263

Meehl, G. A., & Arblaster, J. M. (2002). GCM sensitivity experiments for the Indian monsoon and tropospheric biennial oscillation transition conditions. *Journal of Climate*, *15*(9), 923–944. https://doi.org/10.1175/1520-0442(2002)015<0923:imgset>2.0.co;2

Meehl, G. A., & Arblaster, J. M. (2011). Decadal variability of Asian-Australian monsoon-ENSO-TBO relationships. *Journal of Climate*, *24*(18), 4925–4940. https://doi.org/10.1175/2011jcli4015.1

Meehl, G. A., Arblaster, J. M., Bates, S., Richter, J. H., Tebaldi, C., Gettelman, A., et al. (2020). Characteristics of future warmer base states in CESM2. *Earth and Space Science*, *7*(9). https://doi.org/10.1029/2020EA001296

Meehl, G. A., Arblaster, J. M., & Collins, W. D. (2008). Effects of black carbon aerosols on the Indian monsoon. *Journal of Climate*, *21*(12), 2869–2882. https://doi.org/10.1175/2007jcli1777.1

Meehl, G. A., Shields, C. A., Arblaster, J. M., Neale, R., Hu, A., Annamalai, H., et al. (2023). Climate base state influences on South Asian monsoon processes derived from analyses of E3SMv2 and CESM2. *Geophysical Research Letters*, *50*(17), e2023GL104313. https://doi.org/10.1029/2023GL104313

Mishra, V., Bhatia, U., & Tiwari, A. D. (2020). Bias-corrected climate projections for South Asia from coupled model intercomparison project-6. *Scientific Data*, *7*(1), 338. https://doi.org/10.1038/s41597-020-00681-1

Neale, R. B., Richter, J. H., & Jochum, M. (2008). The impact of convection on ENSO: From a delayed oscillator to a series of events. *Journal of Climate*, *21*(22), 5904–5924. https://doi.org/10.1175/2008JCLI2244.1

Persad, G., Samset, B. H., Wilcox, L. J., Allen, R. J., Bollasina, M. A., Booth, B. B. B., et al. (2023). Rapidly evolving aerosol emissions are a dangerous omission from near-term climate risk assessments. *Environmental Research: Climate*, *2*(3), 032001. https://doi.org/10.1088/2752-5295/acd6af

Petersen, M. R., Asay-Davis, X. S., Berres, A. S., Chen, Q., Feige, N., Hoffman, M. J., et al. (2019). An evaluation of the ocean and sea ice climate of E3SM using MPAS and interannual CORE-II forcing. *Journal of Advances in Modeling Earth Systems*, *11*(5), 1438–1458. https://doi.org/10.1029/2018MS001373

Rajendran, K., Surendran, S., Varghese, S. J., & Sathyanath, A. (2022). Simulation of Indian summer monsoon rainfall, interannual variability and teleconnections: Evaluation of CMIP6 models. *Climate Dynamics*, *58*(9–10), 2693–2723. https://doi.org/10.1007/s00382-021-06027-w

Rasmusson, E. M., & Carpenter, T. H. (1983). The relationship between eastern equatorial Pacific sea surface temperature and rainfall over India and Sri Lanka. *Monthly Weather Review*, *111*(3), 517–528. https://doi.org/10.1175/1520-0493(1983)111<0517:trbeep>2.0.co;2

Roxy, M. K. (2017). Land warming revives monsoon. *Nature Climate Change*, *7*(8), 549–550. https://doi.org/10.1038/nclimate3356

Roxy, M. K., Ritika, K., Terray, P., Murtugudde, R., Ashok, K., & Goswami, B. N. (2015). Drying of Indian subcontinent by rapid Indian Ocean warming and a weakening land-sea thermal gradient. *Nature Communications*, *6*(1), 7423. https://doi.org/10.1038/ncomms8423

Singh, D., Ghosh, S., Roxy, M. K., & McDermid, S. (2019). Indian summer monsoon: Extreme events, historical changes, and role of anthropogenic forcings. *WIREs Climate Change*, *10*(2). https://doi.org/10.1002/wcc.571

Smith, C. J., Kramer, R. J., Myhre, G., Alterskjær, K., Collins, W., Sima, A., et al. (2020). Effective radiative forcing and adjustments in CMIP6 models. *Atmospheric Chemistry and Physics*, *20*(16), 9591–9618. https://doi.org/10.5194/acp-20-9591-2020

Taylor, M. A., Guba, O., Steyer, A., Ullrich, P. A., Hall, D. M., & Eldrid, C. (2020). An energy consistent discretization of the nonhydrostatic equations in primitive variables. *Journal of Advances in Modeling Earth Systems*, *12*(1). https://doi.org/10.1029/2019MS001783

Trenberth, K. E., Dai, A., Rasumssen, R. M., & Parsons, D. B. (2003). The changing character of precipitation. *Bulletin America Meteorology Social*, *84*(9), 1205–1218. https://doi.org/10.1175/BAMS-84-9-1205

Turner, A. G., Inness, P. M., & Slingo, J. M. (2007). The effect of doubled CO_2 and model basic state biases on the monsoon-ENSO system. Part A: Mean response and interannual variability, quarterly. *Journal of the Royal Meteorological Society*, *33*(622), 1143–1157. https://doi.org/10.1002/qj.82

Ueda, H., Iwai, A., Kuwako, K., & Hori, M. E. (2006). Impact of anthropogenic forcing on the Asian summer monsoon as simulated by eight GCMs. *Geophysical Research Letters*, *33*(6), L06703. https://doi.org/10.1029/2005gl025336

Varghese, S. J., Surendran, S., Rajendran, K., & Kitoh, A. (2020). Future projections of Indian Summer Monsoon under multiple RCPs using a high resolution global climate model multiforcing ensemble simulations. *Climate Dynamics*, *54*(3–4), 1315–1328. https://doi.org/10.1007/s00382-019-05059-7

Wang, B., Jin, C., & Liu, J. (2020). Understanding future change of global monsoons projected by CMIP6 models. *Journal of Climate*, *33*(15), 6471–6489. https://doi.org/10.1175/JCLI-D-19-0993.1

Wang, B., et al. (2023). Understanding the recent increase in multiyear La Niñas. *Nature Climate. Change*, *13*, 1075–1081. https://doi.org/10.1038/s41558-023-01801-6

Wu, Q.-Y., Li, Q. Q., Ding, Y. H., Shen, X. Y., Zhao, M. C., & Zhu, Y. X. (2022). Asian summer monsoon responses to the change of land–sea thermodynamic contrast in a warming climate: CMIP6 projections. *Advances in Climate Change Research*, *13*(2), 205–217. https://doi.org/10.1016/j.accre.2022.01.001

Xiang, B., Wang, B., Li, J., Zhao, M., & Lee, J. Y. (2014). Understanding the anthropogenically forced change of equatorial Pacific trade winds in coupled climate models. *Journal of Climate*, *27*(22), 8510–8526. https://doi.org/10.1175/jcli-d-14-00115.1

Yun, K.-S., Lee, J. Y., Timmermann, A., Stein, K., Stuecker, M. F., Fyfe, J. C., & Chung, E. S. (2021). Increasing ENSO-rainfall variability due to changes in future tropical temperature-rainfall relationship. *Communications Earth & Environment*, *2*(1), 43. https://doi.org/10.1038/s43247-021-00108-8

Zhang, G., & Mcfarlane, N. A. (1995). Sensitivity of climate simulations to the parameterization of cumulus convection in the Canadian Climate Centre general circulation model. *Atmosphere-Ocean*, *33*(3), 407–446. https://doi.org/10.1080/07055900.1995.9649539

Zheng, F., Fang, X.-H., Yu, J.-Y., & Zhu, J. (2014). Asymmetry of the Bjerknes positive feedback between the two types of El Niño. *Geophysical Research Letters*, *41*(21), 7651–7657. https://doi.org/10.1002/2014GL062125